Журнал обчислювальної та прикладної математики | 2013, № 3 (113) с. 3–17 | Journal of Computational & Applied Mathematics

UDC 519.6:517.4

NUMERICAL MODELLING OF TEMPERATURE FIELDS DURING IMPULSE FRICTIONAL HARDENING

Ivan Chyr, Heorgiy Shynkarenko

Резюме. Сформульовано початково-крайову та відповідну варіаційну задачу, яка моделює поширення тепла в процесі фрикційного зміцнення деталі рухомим імпульсним поверхневим потоком тепла. На підставі рівняння балансу енергії встановлено умови коректності варіаційної задачі. Дискретизація останньої методом скінченних елеменетів доповнена однокроковою рекурентною схемою інтегрування в часі. Знайдено достатні умови стійкості та збіжності цієї схеми. Запропонована методика ілюструється результатами обчислювальних експериментів, виконаних з використанням середовища FreeFEM++.

Abstract. This paper focuses on the process of detail's frictional hardening with a jagged tool. We state initial boundary value problem for heat conduction in detail under a dynamic impulse heat source and correspondent variational formulation. Conditions for well-posedness of the latter were obtained using the energy balance equation. Finite element space semi-discretization with subsequent one step recurrent time integration scheme were employed. Sufficient conditions for schemes stability and convergence were obtained. Described methodology is illustrated with the results of numerical experiments, implemented using open source environment FreeFEM++.

1. Introduction

Machinery parts play an important role in the exploitation process. They contact between themselves, with other objects and environment. As the main loading of those processes is taken by details surface layers, those physical and chemical properties are directly linked to machine's reliability [9].

Superficial hardening of details results in increase of durability, toughness and the time of their exploitation. We explore the process of superficial hardening with highly concentrated energy source [11]. This energy source is generated in the area of contact between the tool and detail due to friction. During the contact this area is characterized by high increase in temperature and subsequently decrease during its absence [5]. As a result, a special "white" layer with qualitatively better physical and chemical properties is formed.

This paper considers the problem of heat transfer [2] in the workpiece being processed with serrated tool. This will enable us to test general approach to this kind of problems and apply it to the problems of coupled thermo-mechanical fields [8].

Key words. Heat equation, finite element method, mixed problem, impulse moving source, superficial hardening.

It should be mentioned that the problem of heat transfer in technological processes related with hardening is actual and widely considered in technical literature [7, 8].

Main feature of our problem is serration of the tool that produces regime of friction. This property contributes in introducing specific features in the formulation of initial-boundary value problem and needs additional theoretical reasoning during the proof of correctness of its variational form.

So firstly we formulate initial boundary value problem of heat transfer for detail [2]. Main sources of heat in- and outflow are represented with boundary conditions for heat flux in the area of dynamic contact and heat exchange with environment on the rest of details boundary. Then we formulate correspondent variational problem with further Galerkin space semi-discretization. After a little algebra we obtain appropriate Cauchy problem. Based on the properties of the variation problem components we show the uniqueness of its solution. On the next step we build energy equation and derive apriori estimates from the upper limit of linear functional. Consequently, correctness of semi-discrete problem is shown. To finish this whole procedure, we show the correctness of variational problem. This is done on the foundation of the boundness of semi-discrete approximations sequence and apriori estimate of linear functional.

Finally, a time discretization is applied to the semi-discrete problem. Furthermore, sufficient conditions for convergence and stability of resulting one-step time integration recurrent scheme are obtained.

Built numerical scheme was implemented with FreeFEM++ [4] using quadratic finite element approximation. Rates of convergence were verified for the simplest case of our practical problem that includes one contact and contactless periods. Afterwards scheme was applied to model the full process. Resulting data was analyzed and represented with graphs.

2. Statement of the problem

We assume that the workpiece is elastic body which occupies the bounded domain Ω in euclidian space $\Omega \subset \mathbb{R}^d (d = 1, 2, 3)$ with Lipschitz boundary Γ. Let us denote by $x = (x_1, ..., x_d)$ arbitrary point set of the closure $\bar{\Omega} = \Omega \cup \Gamma$ and t is arbitrary moment in time from interval $[0, T]$, $0 < T < +\infty$.

Due to the application of internal heat sources $f = \{f_i(x,t)\}_{i=1}^d$ and surface heat fluxes $\hat{q} = \hat{q}(x,t)$ body temperature changes. These changes are relative to given initial temperature fields $u_0 = u_0(x)$ and will be denoted as $u(x,t)$. Also they satisfy the following heat equation:

$$\rho c_v \frac{\partial u}{\partial t} - \nabla.(\lambda \nabla u) = f \quad in \;\; \Omega \times (0, T], \tag{1}$$

where $\nabla.(\lambda\nabla u) = div\,(\lambda\nabla u)$, $\rho = \rho(x) > 0$ is workpiece density, $c_v = c_v(x) > 0$ is its coefficient of specific heat capacity and $\lambda = \{\lambda_{ij}(x)\}_{i,j=1}^d$ represents matrix of thermal conductivity coefficients that is symmetric and positively defined:

$$\begin{cases} \lambda_{km}(x) = \lambda_{mk}(x), \\ \lambda_{km}(x)\xi_k\xi_m \geq \lambda_0\xi_k\xi_m, \quad \lambda_0 = const > 0, \quad \forall \xi_k \in \mathbb{R} \quad in \quad \Omega, \end{cases} \tag{2}$$

where Einstein summation notation applies.

Equation (1) is supplemented with boundary conditions for interaction with environment, in particular for contact with the tool:

$$-n.(\lambda \nabla u) = \alpha(u - \hat{u})(1 - \delta) + \hat{q}\delta \quad on \quad \Gamma \times [0, T], \tag{3}$$

where $\hat{u} = \hat{u}(x,t)$ is the temperature of environment, $\alpha = \alpha(x,t)$ is heat transfer coefficient and $n = \{n_i\}_{i=1}^{d}$, $n_i = \cos(n, x_i)$ are outer unit normal vector and respectively its components.We also introduce function $\delta(x,t)$ that can accept two values: either 1 for all boundary points in the contact area between tool and detail during the contact period, or 0 in all other cases. Thereby we formulate the following initial boundary value problem:

$$\left\{ \begin{array}{ll} given\ \lambda = \{\lambda_{ij}(x)\}_{i,j=1}^{d},\ \rho = \rho(x),\ c_v = c_v(x), & \\ u_0 = u_0(x),\ \alpha = \alpha(x,t),\ \hat{q} = \hat{q}(x,t),\ f = f(x,t), & \\ \delta = \delta(x,t),\ \hat{u} = \hat{u}(x,t); & \\ find\ temperature\ field\ u = u(x,t),\ such\ that & \\ \rho c_v \frac{\partial u}{\partial t} - \nabla.(\lambda \nabla u) = \rho c_v f & in\ \Omega \times (0, T]\ , \\ -n.(\lambda \nabla u) = \alpha(u - \hat{u})(1 - \delta) + \hat{q}\delta & on\ \Gamma \times [0, T], \\ u|_{t=0} = u_0 & in\ \Omega. \end{array} \right. \tag{4}$$

In addition, we suppose that the data of (4) satisfies the conditions

$$\left\{ \begin{array}{l} \rho, c_v, \lambda_{ij} \in L^{\infty}\left(0, T; L^2(\Omega)\right), \quad u_0 \in L^2(\Omega), \\ f \in L^2\left(0, T; L^2(\Omega)\right), \quad \alpha, \delta \in L^{\infty}\left(0, T; L^2(\Gamma)\right), \\ \hat{u}, \hat{q} \in L^2\left(0, T; L^2(\Gamma)\right). \end{array} \right. \tag{5}$$

3. Variational formulation

To formulate a variational problem, let us introduce spaces of admissible temperatures $V = H^1(\Omega)$, conjugated space V' and spaces $H = L^2(\Omega)$.

Hereinafter we will use the following notation

$$u(t) = u(x,t) - \quad function\ x \to u(x,t),$$
$$u'(t) = \partial u / \partial t - \quad function\ x \to \frac{\partial u(x,t)}{\partial t}.$$

Let us multiply heat equation of system (4) by arbitrary function $v \in V$ with successive integration over Ω. After utilization of Green's formula and boundary condition (3) we obtain

$$\begin{aligned} 0 &= \int_{\Omega} \{\rho c_v u'(t) - \nabla.[\lambda \nabla u(t)] - f(t)\} v dx = \int_{\Omega} \rho c_v u'(t) v dx \\ &+ \int_{\Omega} (\nabla v).[\lambda \nabla u(t)] dx - \int_{\Omega} f(t) v dx + \int_{\Gamma} \alpha(t) u(t)[1 - \delta(t)] v d\gamma \\ &- \int_{\Gamma} \alpha(t) \hat{u}(t)[1 - \delta(t)] v d\gamma - \int_{\Gamma} \hat{q}(t) \delta(t) v d\gamma. \end{aligned} \tag{6}$$

As the next step, we introduce the following bilinear forms

$$s(u,v)=\int_{\Omega}\rho c_v uvdx \qquad \forall u,v\in H, \tag{7}$$

$$a(u,v)=\int_{\Omega}(\nabla v).[\lambda\nabla u]dx+\int_{\Gamma}\alpha u[1-\delta]vd\gamma \qquad \forall u,v\in V, \tag{8}$$

and such linear functional

$$<l,v>=\int_{\Omega}\rho c_v f vdx+\int_{\Gamma}[\alpha\hat{u}(1-\delta)+\hat{q}\delta]vd\gamma \qquad \forall v\in V. \tag{9}$$

Thus the variatinal formulation of (4) can be represented in the following manner:

$$\left\{\begin{array}{l} find\ \ such\ \ heat\ \ distribution\ u(x,t)\ that \\ s(u'(t),v)+a(u(t),v)=<l(t),v> \quad \forall v\in V,\ \ \forall t\in(0,T], \\ s(u(0)-u_0,v)=0. \end{array}\right. \tag{10}$$

4. Properties of the variational problem components

From definition of bilinear forms we can state the following

$$\left\{\begin{array}{l} symmetric\ \ continous\ bilinear\ \ form\ \ s\left(\cdot,\cdot\right)\ \ defined\ by\ (3) \\ is\ \ H-elliptic\ and\ generates\ \ norm\ \|u\|_H=s^{\frac{1}{2}}\left(u,u\right) \qquad \forall u\in H, \\ which\ is\ equivalent\ to\ \ \|\cdot\|_{0,\Omega}\,. \end{array}\right. \tag{11}$$

Second bilinear form has more complex structure that results is necessity of additional confirmation of its properties.

Theorem 1. *Let conditions* (5) *and* (2) *are satisfied.*

Then bilinear form $a(\cdot,\cdot)$ *defined by* (8) *is continuous and the following inequality holds*

$$|a(u,v)|\leq C\left[\|\lambda\|_{L^\infty(\Omega)}+\|\alpha\|_{L^\infty(\Gamma)}\right]\|u\|_{H^1(\Omega)}\|v\|_{H^1(\Omega)}.$$

Proof. Using Cauchy-Bunyakovsky-Schwarz inequality and trace theorem [10, p. 72-73] we obtain

$$\begin{aligned} |a(u,v)| &\leq |\int_{\Omega}(\lambda\nabla u)\,.\,(\nabla v)\,dx|\ +|\int_{\Gamma}\alpha u(1-\delta)vd\gamma| \\ &\leq \int_{\Omega}|\lambda\nabla u|.|\nabla v|dx+\int_{\Gamma}|\alpha uv|d\gamma \leq \{\int_{\Omega}|\lambda\nabla u|^2dx\int_{\Omega}|\nabla v|^2dx\}^{\frac{1}{2}} \\ &+\{\int_{\Gamma}|\alpha u|^2|v|^2d\gamma\}^{\frac{1}{2}} \leq \|\lambda\nabla u\|_H\|\nabla v\|_H+\|\alpha u\|_{L^2(\Gamma)}\|v\|_{L^2(\Gamma)} \\ &\leq C\left[\|\lambda\|_{L^\infty(\Omega)}+\|\alpha\|_{L^\infty(\Gamma)}\right]\|u\|_{H^1(\Omega)}\|v\|_{H^1(\Omega)}, \qquad \forall u,v\in H^1(\Omega). \end{aligned}$$

This means that $a(\cdot,\cdot)$ is bounded and as a result continuous. □

Theorem 2. *Let conditions* (5) *and* (2) *are satisfied.*

Bilinear form $a(\cdot,\cdot)$ *defined by* (8) *is* $H^1(\Omega)-$ *elliptic, moreover the following inequality holds:*

$$a(u,u) \geq m_0 \frac{\min\{1, C_F\}}{2} \|u\|^2_{H^1(\Omega)} .$$

Proof. The latter estimation can be obtained after utilization of Friedrichs inequality and the following transmutations

$$\begin{aligned}
&a(u,u) \geq \lambda_{\max} \int_\Omega (\nabla u)^2 dx + \int_\Gamma \alpha u^2 (1-\delta) d\gamma \\
&\geq \min\{\lambda_{\max}, \alpha_0\} \left[\int_\Omega (\nabla u)^2 dx + \int_\Gamma u^2 d\gamma \right] \\
&\geq \min\{\lambda_{\max}, \alpha_0\}[\tfrac{1}{2}(\int_\Omega (\nabla u)^2 dx + \int_\Gamma u^2 d\gamma) + \tfrac{1}{2}(\int_\Omega (\nabla u)^2 dx + \int_\Gamma u^2 d\gamma)] \\
&\geq \mathrm{m}_0 \left[\tfrac{1}{2} \int_\Omega (\nabla u)^2 dx + \tfrac{C_F}{2} \int_\Omega u^2 dx \right] \geq m_0 \frac{\min\{1, C_F\}}{2} \|u\|^2_{H^1(\Omega)} .
\end{aligned}$$

□

Corollary 1. *Let conditions* (5) *and* (2) *are satisfied then following statement holds:*

$$\left\{ \begin{array}{l} symmetrical\ continuous\ bilinear\ form\ a(\cdot,\cdot)\ from\ (2.4) \\ is\ V-elliptic\ and\ generates\ norm\ \|u\|_V = a^{\frac{1}{2}}(u,u)\ \ \forall u \in V, \\ which\ is\ equivalent\ to\ \|\cdot\|_{1,\Omega}. \end{array} \right. \qquad (12)$$

Finally, let us derive the upper estimation of linear functional (9). This is done starting with application of Cauchy-Bunyakovsky-Schwarz inequality and theorem [10, p. 72-73] about the trace of the function from $H^1(\Omega)$ on the boundary of Ω

$$\begin{aligned}
&|< l, v >| = \left| \int_\Omega \rho c_v f v dx + \int_\Gamma \alpha \hat{u} (1-\delta) v d\gamma + \int_\Gamma \hat{q} \delta v d\gamma \right| \\
&\leq ||\rho c_v||_{\infty,\Omega} ||f||_H ||v||_H + ||\alpha||_{\infty,\Gamma} ||\hat{u}||_{L^2(\Gamma)} ||v||_{L^2(\Gamma)} + ||\hat{q}||_{L^2(\Gamma)} ||v||_{L^2(\Gamma)} \\
&\leq [\, ||\rho c_v||^2_{\infty,\Omega} ||f||^2_H + ||\alpha||^2_{\infty,\Gamma} ||\hat{u}||^2_{L^2(\Gamma)} + ||\hat{q}||^2_{L^2(\Gamma)}]^{1/2} [||v||^2_H + 2||v||^2_{L^2(\Gamma)}]^{1/2} \\
&\leq C \max\{\, ||\rho c_v||_{\infty,\Omega}, ||\alpha||_{\infty,\Gamma}, 1\} [||f||^2_H + ||\hat{u}||^2_{L^2(\Gamma)} + ||\hat{q}||^2_{L^2(\Gamma)}]^{1/2} ||v||_V \\
&\hspace{30em} \forall v \in V.
\end{aligned}$$

This reasoning results in the following statement.

Theorem 3. *Linear functional* $< l, v >$ *defined by* (9) *in continuous and satisfies the following estimation*

$$|< l, v >| \leq z_0 [||f||^2_H + ||\hat{u}||^2_{L^2(\Gamma)} + ||\hat{q}||^2_{L^2(\Gamma)}]^{1/2} ||v||_V \qquad \forall v \in V,$$

where $z_0 = C \max\{\, ||\rho c_v||_{\infty,\Omega}, ||\alpha||_{\infty,\Gamma}, 1\}$.

5. Galerkin semi-discretization

To calculate approximate solutions of variational problem (10) we select sequence of finite element subspaces $\{V_h\} \subset V$ such that $\dim V_h = N(h) = N \to +\infty$ and $\bigcup\limits_{h>0} V_h$ is complete in V. Then for any $h > 0$ we gain the following semi-discrete approximations of the variational problem (10)

$$\left\{ \begin{array}{ll} given\ u_0 \in V; find\ u_h(x,t) \in L^2(0,T;V_h)\ such\, that & \\ s(u'_h(t), v) + a(u_h(t), v) = < l(t), v > & \forall t \in (0,T], \\ s(u_h(0) - u_0, v) = 0 & \forall v \in V_h. \end{array} \right. \tag{13}$$

Next we denote by $\{\varphi_i\}_{i=1}^N$ the basis of the space V_h. Consequently sought solution of (13) will take form of the following linear combination

$$u_h(x,t) = \sum\nolimits_{m=1}^N U_m(t)\varphi_m(x) \tag{14}$$

with unknown coefficients $U_1(t), ..., U_N(t)$. Substitution of (14) into (13) yeilds such problem

$$\left\{ \begin{array}{l} given\ u_0 \in V; find\, u_h(x,t) \in L^2(0,T;V_h)\ such\, that \\ \sum_{m=1}^N U'_m(t) s(\varphi_m(x), v) + \sum_{m=1}^N U_m(t) a(\varphi_m(x), v) \\ \qquad\qquad = < l(t), v > \quad \forall t \in (0,T], \\ \sum_{m=1}^N U_m(0) s(\varphi_m(x), v) = s(u_0, v) \qquad \forall v \in V_h. \end{array} \right. \tag{15}$$

This problem can be transformed into Cauchy problem after consequent substitution of $v = \varphi_i$, $i = 1, ..., N$, into (15). As a result, we receive the following equations.

$$\left\{ \begin{array}{ll} SU'(t) + AU(t) = R(t) & \forall t \in (0,T], \\ SU(0) = S^0. & \end{array} \right. \tag{16}$$

Statements (11), (12) show that matrices S and A are Gramians of linearly independent functions $\{\varphi_i\}_{i=1}^N$ respectively to scalar products $s(\cdot,\cdot)$ and $a(\cdot,\cdot)$. Thus

$$\left\{ \begin{array}{l} symmetrical\ \ matrices \\ S = \{s(\varphi_i,\varphi_j)\}_{i,j=1}^N, \quad A = \{a(\varphi_i,\varphi_j)\}_{i,j=1}^N \\ are\ \ positively\ \ defined. \end{array} \right. \tag{17}$$

Since data of the problem (4) satisfies regularity conditions (5) and (17) holds, Cauchy problem (16) has unique solution.

6. Energy equation

Special kind of equation can be obtained from (13) after assuming that $v = u_h(t)$:

$$\left\{ \begin{array}{l} \frac{1}{2}\frac{d}{dt}[s(u_h(t), u_h(t))] + a(u_h(t), u_h(t)) \\ \qquad\qquad = < l(t), u_h(t) > \quad \forall t \in (0,T], \\ s(u_h(0), u_h(0)) = s(u_0, u_h(0)). \end{array} \right. \tag{18}$$

If we take into account (11), (12), the latter system can be reformulated in such a manner

$$\begin{cases} \frac{1}{2}\frac{d}{dt}\left\|u_h(t)\right\|_H^2 + \left\|u_h(t)\right\|_V^2 =< l(t), u_h(t) >, \\ \left\|u_h(0)\right\|_H^2 = s(u_0, u_h(0)). \end{cases} \tag{19}$$

The first equation of (19) can be integrated over $[0,t]$ to get such equality:

$$\frac{1}{2}\left\|u_h(t)\right\|_H^2 + \int_0^t \left\|u_h(\tau)\right\|_V^2 d\tau = \frac{1}{2}\left\|u_h(0)\right\|_H^2 + \int_0^t < l(\tau), u_h(\tau) > d\tau \qquad \forall t \in [0,T]. \tag{20}$$

It should be noted that the last equality is the basis for further proof of well-posedness of (10). Futhermore, left part of (20) is natural (energy) norm for this problem.

7. Apriori estimates and well-posendess of variational problem

Now we can apply Cauchy-Shwarz inequality to the right part of (20) to calculate such an estimate

$$\begin{aligned} \left|\int_0^t < l(\tau), u_h(\tau) > d\tau\right| &\le \int_0^t ||l(\tau)||_* ||u_h(\tau)||_V d\tau \\ &\le \tfrac{1}{2}\int_0^t [\,||l(\tau)||_*^2 + ||u_h(\tau)||_V^2]\, d\tau \end{aligned} \tag{21}$$

Hence, utilizing equation (20) and inequality (21), we obtain

$$\tfrac{1}{2}\left\|u_h(t)\right\|_H^2 + \int_0^t \left\|u_h(\tau)\right\|_V^2 d\tau \le \tfrac{1}{2}\left\|u_h(0)\right\|_H^2 + \tfrac{1}{2}\int_0^t [\,||l(\tau)||_*^2 + ||u_h(\tau)||_V^2]\, d\tau$$

which can be rewritten into

$$\left\|u_h(t)\right\|_H^2 + \int_0^t \left\|u_h(\tau)\right\|_V^2 d\tau \le \left\|u_h(0)\right\|_H^2 + \int_0^t ||l(\tau)||_*^2 \, d\tau \quad \forall t \in [0,T]. \tag{22}$$

Consequently this states that

$$\begin{cases} semi-discrete\ Galerkin\ approximations\ \{u_h\} \\ form\ a\ bounded\ set\ in\ space\, L^\infty\left(0,T;H\right) \cap L^2\left(0,T;V\right). \end{cases} \tag{23}$$

This also states the stability of semi-discrete approximations.

Theorem 4. *Given fixed $h > 0$ and $\{\varphi_i\}_{i=1}^N$, the basis of V_h. Then semi-discrete problem* (13) *allows a unique solution $u_h \in L^\infty\left(0,T;H\right) \cap L^2\left(0,T;V\right)$ that is uniquely defined by Cauchy problem* (16) *and decomposition* (14). *Moreover inequality* (22) *holds.*

Corollary 2. *For each $h > 0$ the semi-discrete problem* (13) *is well-posed.*

Theorem 5. *Given $u_0 \in H,\ l \in L^2\left(0,T;V'\right)$. Then variational problem (3.6) has unique solution $u \in L^\infty\left(0,T;H\right) \cap L^2\left(0,T;V\right)$ and $u' \in L^2\left(0,T;V'\right)$. Furthermore $(l, u_0) \to u$ is continuous mapping from $L^2\left(0,T;V'\right) \times H$ into $L^2\left(0,T;V'\right) \cap L^\infty\left(0,T;H\right)$.*

Proofs of these theorems can be found e.g. in [12, pp. 44-45].

8. One-step time integration recurrent scheme

To construct a numerical scheme for solving a variational problem (10) we also need to discretize problem (13) in time. To accomplish this we use projection method. In this section we will omit index h for simplicity of notation.

Let us divide time interval $[0,T]$ into P subintervals $[t_k, t_{k+1}]$, $k = 0,..,P-1$, with the constant length $\Delta t = t_{k+1} - t_k > 0$. On every time step $[t_k, t_{k+1}]$, $k = 0,...,P-1$, solution $u_h(t) \in V_h$ of (13) will be approximated by polynomial function $u_{\Delta t}(t)$ such that

$$\begin{aligned} &u_{\Delta t}(t) = [1-\omega(t_j,t)]u^j + \omega(t_j,t)u^{j+1}, \\ &\omega(t_j,t) = (t-t_j)/\Delta t, \qquad t \in [t_j,t_{j+1}],\ j = 0,...,P-1. \end{aligned} \tag{24}$$

The latter function can be rewritten in the following manner:

$$\begin{aligned} &u_{\Delta t}(t) = u^j + \Delta t\omega(t_j,t)\tfrac{u^{j+1}-u^j}{\Delta t} \\ &= \tfrac{1}{2}(u^{j+1}+u^j) + \Delta t(\omega(t_j,t)-\tfrac{1}{2})\tfrac{u^{j+1}-u^j}{\Delta t} \\ &= u^{j+1/2} + \Delta t(\omega(t_j,t)-\tfrac{1}{2})\dot{u}^{j+1/2}, \quad \dot{u}^{j+1/2} = (u^{j+1}-u^j)/\Delta t. \end{aligned} \tag{25}$$

Linear functional will be approximated with piecewise-constant functions:

$$l_{\Delta t}(t) = l_{j+1/2} = l(t_{j+1/2}), \qquad t_{j+1/2} = t_j + \tfrac{1}{2}\Delta t. \tag{26}$$

Summing assumptions (25) and (26) and consequent substitution into (13) yields:

$$\left\{ \begin{aligned} &find\ \dot{u}^{j+1/2}, u^{j+1} \in V_h\ such\,that \\ &s(\dot{u}^{j+1/2},v) + \Delta t\omega(t_j,t)a(\dot{u}^{j+1/2},v) \\ &\qquad =< l_{j+1/2}, v > -a(u^j,v), \\ &u^{j+1} = u^j + \Delta t\dot{u}^{j+1/2}, \quad \forall v \in V_h,\ \forall t \in [t_j,t_{j+1}], \\ &s(u^0 - u(0),v) = 0, \qquad j = 0,...,P-1. \end{aligned} \right. \tag{27}$$

The next phase is construction of projective equations. Here we denote by $(\cdot,\cdot)$ a scalar product in space $L^2((t_j,t_{j+1}))$ and choose in it function $\xi(t)$ such that

$$(\xi,1) = \int_{t_j}^{t_{j+1}} \xi(t)dt = 1.$$

We introduce notation $\theta = (\omega,\xi)$ and assume that (27) is orthogonal to function $\xi(t)$ with respect to scalar product $(\cdot,\cdot)$ or in other terms:

$$\begin{aligned} &s(\dot{u}^{j+1/2},v) + \Delta t\theta a(\dot{u}^{j+1/2},v) =< l_{j+1/2}, v > -a(u^j,v), \\ &\qquad \forall v \in V_h, \quad j = 0,...,P-1, \quad \forall \theta \in [0,1]\ . \end{aligned}$$

As a result we can denote the following one-step time-integration recurrent scheme (hereinafter denoted as ORS):

$$\begin{cases} given\ \theta \in [0,1]\,,\ u^0; find\ \dot{u}^{j+1/2}, u^{j+1} \in V_h\, such\, that \\ s(\dot{u}^{j+1/2}, v) + \Delta t\theta a(\dot{u}^{j+1/2}, v) =< l_{j+1/2}, v > -a(u^j, v), \\ u^{j+1} = u^j + \Delta t\dot{u}^{j+1/2} \qquad \forall v \in V_h, \\ s(u^0 - u(0), v) = 0 \qquad j = 0, ..., P-1. \end{cases} \tag{28}$$

Taking into account the $H-$ and $V-$ellipticity of bilinear forms $s\,(\,\cdot\,,\,\cdot\,)$ and $a\,(\,\cdot\,,\,\cdot\,)$ and also Lax-Milgram-Vyshyk lemma [1], ORS (28) is uniquely solved with respect to u^0, $\dot{u}^{j+1/2}$ and u^{j+1}.

In such manner, piecewise-linear approximation $u_{h\Delta t}\,(t) \in V_h$ of (13) solution $u_h\,(t) \in V_h$ is uniquely determined after application of scheme (28).

Stability and convergence of ORS must also be considered.

Theorem 6. *If data of variational problem* (10) *fulfill* (4), *the ORS scheme* (28) *with parameters* Δt *and* θ *is:*

1. *unconditionally (with respect to chosen* Δt*) stable in spaces* H *and* V*, when* $\theta \geq \frac{1}{2}$*;*
2. *stable in spaces* H *and* V*, when parameter* Δt *meets inequality:*

$$\Delta t \leq \frac{2}{\alpha\,(1-2\theta)}.$$

Theorem 7. *Let the solution* $u_h\,(t)$ *of problem* (12) *is such that* $u_h{}''' \in C\,(0, T; V)$ *and let* $u_{h\Delta t}\,(t)$ *is his piecewise-linear approximation, obtained with application of unconditionally stable scheme* (28) *with parameter* $\theta \geq \frac{1}{2}$.

Then the sequence $u_{h\Delta t}$*, with respect to enery norm*

$$\|u\|_T^2 = \tfrac{1}{2}\,\|u(T)\|_{H^0(\Omega)}^2 + \int_0^T \|\nabla u(t)\|_{H^0(\Omega)}^2\,dt,$$

converges to u*, when* $\Delta t \to 0$ *and* $h \to 0$.

Proofs of theorems 6, 7 and analisys of space and temporal error convergence rates can be found e.g. in [12].

9. Validation of numerical scheme

Sheme (28) can be implemented in the majority of specialized environments. So for testing of numerical scheme we used a free, open source environment FreeFEM++, with quadratic triangular finite elements, due to simplicity of problem description, ability to work with resulting matrices and near optimal execution speed [4].

Taking into account that the analytical solution of problem (4) is not known, we will only examine a posteriori rates of convergence of finite element scheme.

Our two-dimensional model problem will be formed as (4) with the following characteristics:

$$l = 41 \cdot 10^{-4}\ [m], \qquad b = 55 \cdot 10^{-5}\ [m], \qquad T = 56 \cdot 10^{-5}\ [s], \quad x_c = 0\ [m],$$

$$t_c = 48 \cdot 10^{-5}\ [s], \qquad \widehat{q} = 8.2 \cdot 10^6\ \ [W/m^2], \quad \rho = 7850\ [kg/m^3],$$

$$c_V = 466\ [J/(kg\cdot K)],\qquad \lambda = 41\ [W/(m\cdot K)],\ \ \alpha = 500\ \ [W/(m^2\cdot K)],$$
$$v_h = 4\ \ [m/s],\qquad v_d = 60\ \ [m/s],\qquad n_z = 24,\qquad l_c = 3\cdot 10^{-3}\ [m].$$

where l is the length and b is thickness of workpiece. Given that $\Omega = (0,l)\times(0,b)$ we can concretize function $\delta(x,t)$ from (4) in the following manner :

$$\delta(x,t) = \begin{cases} 1, x\in\gamma(t),\ \ t\in[t_{k-1},t_k],\ \ t-t_k <= t_c, \\ 0, t-t_k > t_c, \end{cases} \qquad k = 1,..,N,$$

where $\gamma(t) = \{(x_1,x_2) : x_1 \in [v_h t - l_c/2 + x_c, v_h t + l_c/2 + x_c], x_2 = b\}$ is area of dynamic contact, t_k is the initial time of k contact, t_c is time of single tooth contact, l_c is length of contact zone, x_c represents the initial displacement of the contacts area and v_h represents the velocity of contact zone.

For verification of approximate solutions accuracy we will evaluate rates of convergence separately for space and time discretization in the following norms (as in [13]) :

$$\begin{aligned} &\|u\|^2_{H^m(\Omega)} = \|u\|^2_m = \sum\nolimits_{|\alpha_1+\alpha_2|\le m} \int_\Omega \Big(\frac{\partial^{\alpha_1+\alpha_2}}{\partial {x_1}^{\alpha_1}\partial {x_2}^{\alpha_2}}u\Big)^2 dx, \\ &\|u\|^2_T = \tfrac{1}{2}\,\|u(T)\|^2_{H^0(\Omega)} + \int_0^T \|\nabla u(t)\|^2_{H^0(\Omega)}\,dt. \end{aligned} \tag{29}$$

Introduction of these norms enables us to calculate the following indicators of convergence rates:

$$\begin{aligned} &p^m_{\Delta t}(u) = \log_2\frac{\|u_{\Delta t} - u_{\Delta t/2}\|_m}{\|u_{\Delta t/2} - u_{\Delta t/4}\|_m}, \quad p_{\Delta t}(u) = \log_2\frac{\|u_{\Delta t} - u_{\Delta t/2}\|_T}{\|u_{\Delta t/2} - u_{\Delta t/4}\|_T}, \\ &p^m_h(u) = \log_2\frac{\|u_h - u_{h/2}\|_m}{\|u_{h/2} - u_{h/4}\|_m}, \qquad p_h(u) = \log_2\frac{\|u_h - u_{h/2}\|_T}{\|u_{h/2} - u_{h/4}\|_T}. \end{aligned} \tag{30}$$

10. Convergence of spatial approximations

We use sequence of uniformly refined triangulations $\mathcal{T}_h$ of isosceles triangles to determine convergence rates with respect to space variables, where $T_h = \{K\},\ h_K = diam\, K = \sqrt{2}\frac{b}{N}$, where N is the number of divisions of smaller side b of Ω . Results are obtained at time T with time step $\Delta t = \frac{T}{224} = 2,5\cdot 10^{-7}\ [s]$.

For analysis of convergence we utilize norms (29) and the following indicators of absolute and relative errors

$$\begin{aligned} &e^m_h(u) = \|u_h - u_{h/2}\|_m, \qquad \varepsilon^m_h(u) = \frac{\|u_h - u_{h/2}\|_m}{\|u_{h/2}\|_m}\times 100\,\%, \\ &e_h(u) = \|u_h - u_{h/2}\|_T, \qquad \varepsilon_h(u) = \frac{\|u_h - u_{h/2}\|_T}{\|u_{h/2}\|_T}\times 100\,\%. \end{aligned} \tag{31}$$

Given that we use quadratic finite element approximations, theoretically rates of convergence for given spaces are $p^0_h(u) = 3$, $p^1_h(u) = 2$ and $p_h(u) = 1$. Acquired results indicate ability of ORS to converge with required rates. It should be noted that application of norm $\|\cdot\|_T$ gives ability to protect

TABL. 1. Convergence of spacial approximations in norms (29)

N	$e_h^0(u)\cdot 10^{-3}$	$e_h^1(u)$	$e_h(u)$	$p_h^0(u)$	$p_h^1(u)$	$p_h(u)$	$\varepsilon_h^0(u)$	$\varepsilon_h^1(u)$	$\varepsilon_h(u)$
1/7	4,22	158,08	5,15	1,49	0,47	0,45	0,92	39,74	39,77
1/14	1,94	122,18	2,71	1,12	0,37	0,92	0,42	31,06	20,77
1/28	0,41	31,88	1,18	2,23	1,94	1,20	0,09	8,08	9,02
1/56	0,04	7,30	0,48	3,30	2,13	1,29	0,01	1,85	3,70

against accidental measurements in "well-suited" time and represents accumulation of special discretization error during preceding period.

11. CONVERGENCE IN TIME

To verify convergence in time we fix space mesh with initial parameters 256×64 and examine the nature of a posteriori rates of convergence during successive refinement of time step $\Delta t = T/P$.

We also use the following indicators for this analysis:

$$\begin{aligned} e_{\Delta t}^m(u) &= \left\|u_{\Delta t} - u_{\Delta t/2}\right\|_m, & \varepsilon_{\Delta t}^m(u) &= \frac{\left\|u_{\Delta t} - u_{\Delta t/2}\right\|_m}{\left\|u_{\Delta t/2}\right\|_m} \times 100\,\%, \\ e_{\Delta t}(u) &= \left\|u_{\Delta t} - u_{\Delta t/2}\right\|_T, & \varepsilon_{\Delta t}(u) &= \frac{\left\|u_{\Delta t} - u_{\Delta t/2}\right\|_T}{\left\|u_{\Delta t/2}\right\|_T} \times 100\,\%. \end{aligned} \tag{32}$$

TABL. 2. Convergence in time of solution in terms of norms (29)

P	$e_{\Delta t}^0(u)\cdot 10^{-3}$	$e_{\Delta t}^1(u)$	$e_{\Delta t}(u)$	$p_{\Delta t}^0(u)$	$p_{\Delta t}^1(u)$	$p_{\Delta t}(u)$	$\varepsilon_{\Delta t}^0(u)$	$\varepsilon_{\Delta t}^1(u)$	$\varepsilon_{\Delta t}(u)$
56	2,73	453,85	6,38	1,99	1,53	0,74	0,59	102,82	46,78
112	0,69	157,31	3,81	1,31	0,81	0,83	0,15	38,56	28,67
224	0,28	89,71	2,14	2,03	1,80	1,01	0,06	22,71	16,33
448	0,07	25,76	1,06	1,62	5,91	1,09	0,01	6,53	8,12

Based on these results we state that scheme (28) achieves theoretical rates of convergence in time. As we use Crank-Nicolson scheme for time integration $p_{\Delta t}^0(u)$, $p_{\Delta t}^1(u)$ must be greater or equal to 2 and $p_{\Delta t}(u)$ this number is 1.

Acquired numerical results indicate the correctness of used ORS scheme and its potential for practical utilization.

12. NUMERICAL EXPERIMENTS

As our paper also concerns practical experiment we modeled the process of frictional hardening for detail with such parameters:

$$l = 44 \cdot 10^{-4}\ [m], \qquad b = 65 \cdot 10^{-5}\ [m]$$

Workpiece is made of steel (Stal-45) which has the following properties:

$$\rho = 7850\ [kg/m^3], \qquad c_V = 466\ [J/(kg \cdot K)], \qquad \lambda = 41\ [W/(m \cdot K)].$$

In the initial time it is heated to the temperature of $\hat{u} = 293\ [^\circ,\ K]$. It is rigidly fixed on the table that moves with linear speed $v_h = 4\ [m/s]$. Points on tools surface circulate with speed $v_d = 60\ [m/s]$. Tool-workpiece interaction creates a contact zone $l_c = 3 \cdot 10^{-3}$ $[m]$ in length causing a heat source with the power of $\widehat{q} = 8.2 \cdot 10^7$ $[W/m^2]$ to be generated. Due to serration of tool's surface contact (and subsequently heat source) has a special periodic regime. Also we assume that one contact lasts for $t_c = 48 \cdot 10^{-5}$ $[s]$, one contactless period is $t_p = 8 \cdot 10^{-5}$ $[s]$ and $x_c = -1.5\, l_c$ $[m]$.

To complete the description of technological process we should mention that the cooling liquid is supplied to the contact area. The heat transfer coefficient between workpiece and coolant is $\alpha = 500$ $[W/(m^2 \cdot K)]$. We also consider time $T = 280 \cdot 10^{-5}$ $[s]$ that covers full processing of the workpiece. In the initial moment of time the tool is situated aside of the detail. As experiment begins it starts to move in the direction of detail.

As a result of numerical experiment, the following graphics of temperature distribution were obtained (Fig. 1). They represent state of temperature field in different times so one can see the dynamics of the process.

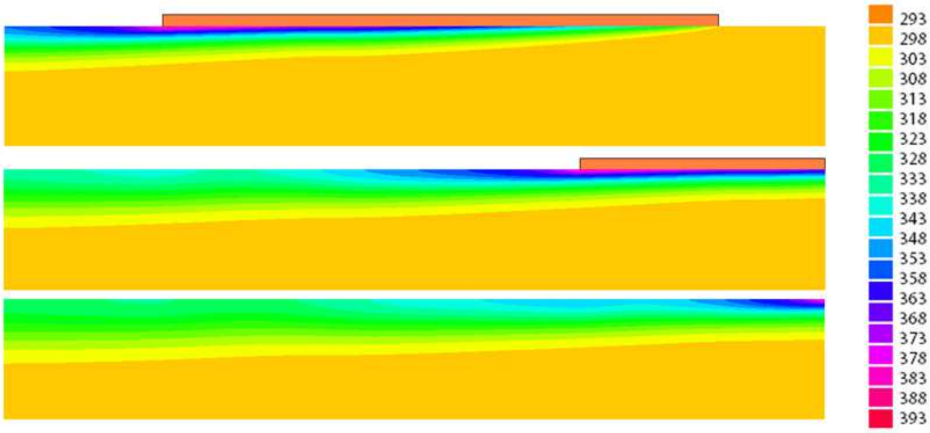

FIG. 1. Distribution of temperature after contact with the second, third and fourth tooth of the tool (respectively first, second and third figure from the top). Contact area is depicted with a rectangle

Also special attention was drawn to evolution of maximal temperature that clearly shows the influence of serration of tool's surface into technological process (Fig. 2).

Latter characteristic is aggregative and incomplete without full knowledge of the place where this maximum occurs. As the maximum is reached on contact surface we supply figures to show the evolution on temperature profile on it (Fig. 3). Also to be noted that stripes in the background of these figures represent the area of dynamic contact in corresponding points in time.

These figures shed a light on singularities of the temperature profile evolution on the contact surface. First figure shows the last moment of the first contact. Figure b illustrates temperature decrease and creation of unheated area. Then second tooth starts to act and finishes with surface heated to temperature as

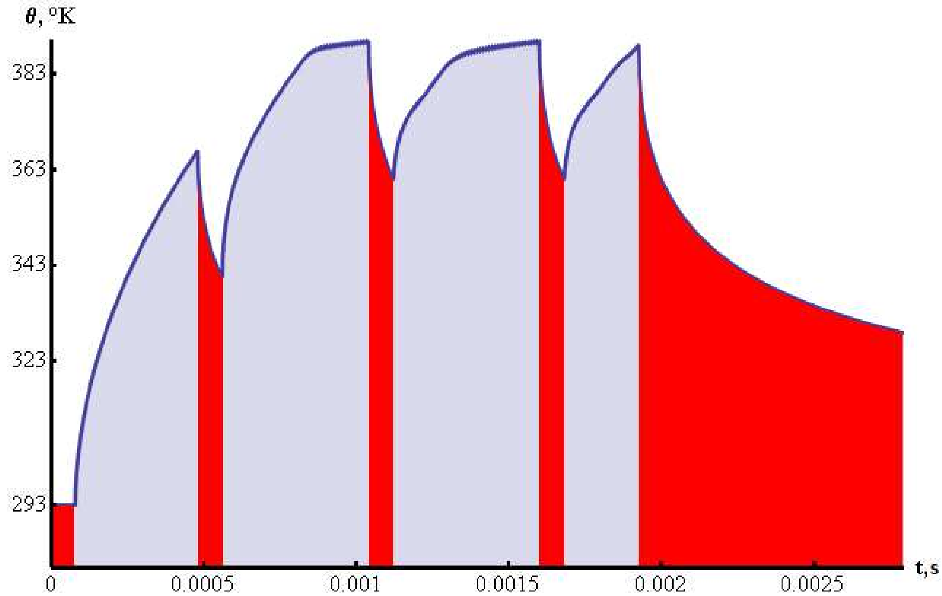

FIG. 2. Evolution of maximal temperature during the experiment with highlighted contactless intervals

can be seen of figure d. The following figures demonstrate further evolution of heat profile on the surface.

These figures reveal interesting singularities of examined problem. Illustrations depict that the speed of heat conduction is less than the speed of contact area. If we write down the corresponding ration in dimensionless form, we obtain the Peclet number for a specific problem [11, p.12]:

$$Pe = v_h \cdot l_d \cdot (\lambda / c_V \rho)^{-1} \approx \frac{4 \cdot 0,003}{1{,}121 \cdot 10^{-5}} \approx 1070$$

Given the magnitude of this characteristic (singularly unperturbed problems have $Pe < 10$) we can state that this problem is singularly perturbed.

13. Conclusions

In the process of research the initial boundary value problem for the heat conduction process in workpiece during friction hardening was stated. Successively we formulated correspondent variational problem and proved its welposendess. With utilization of Poincare-Freidrich's inequality a V-ellipticity of bilinear form with term from boundary condition for heat exchange with environment was proven. This gave opportunity to extend known result (e.g. [12, pp. 29-62]) to our problem.

Modeling of the frictional hardening with a jagged tool brings in some difficulties related to its mathematical model. They show themselves in form of mixed boundary conditions. Moreover due to magnitude of Peclet number, investigated problem is singularly perturbed. This fact will also contribute

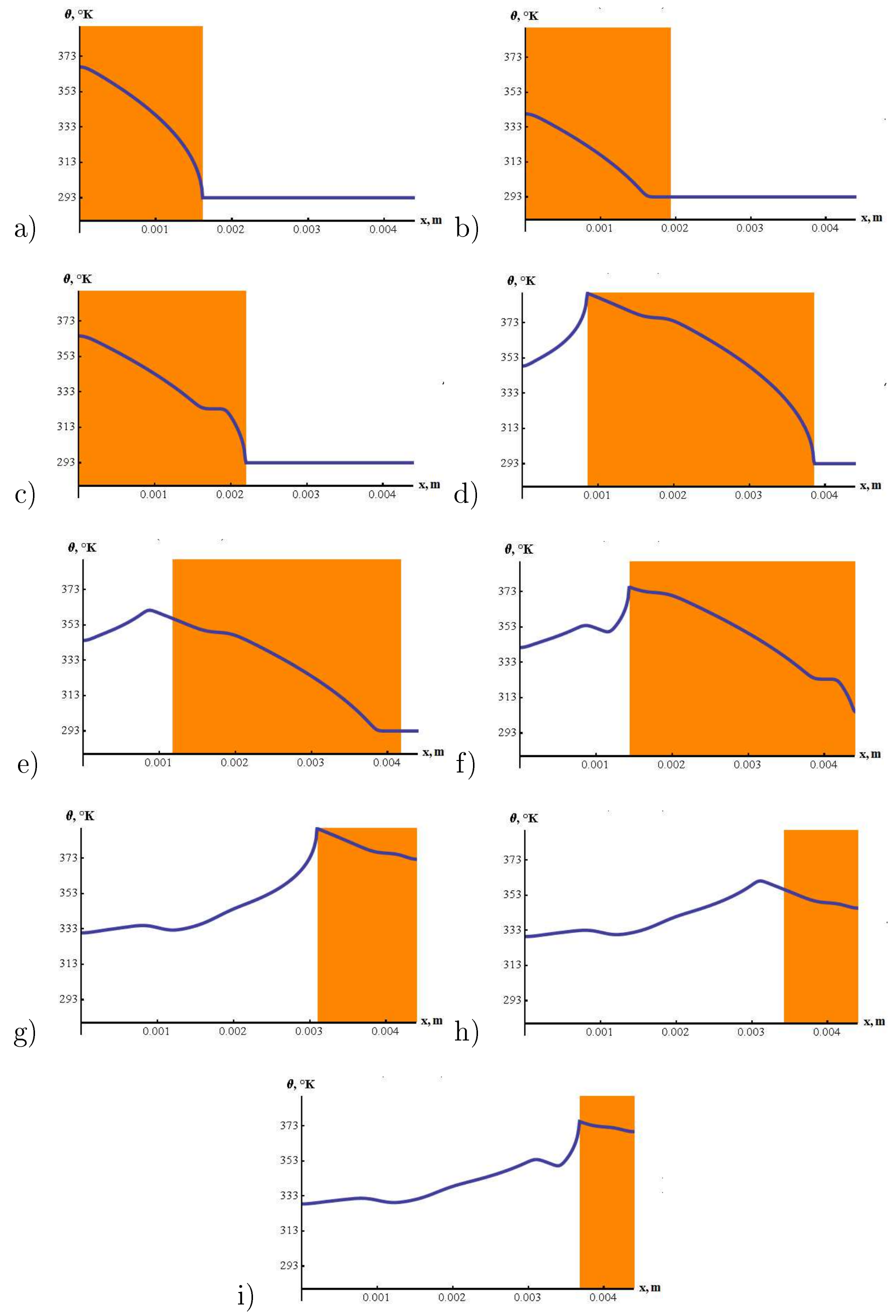

FIG. 3. The distribution of temperature on the contact surface at a) 0.00048 s, b) 0.00055875 s, c) 0.000625 s, d) 0.00104 s, e) 0.00111875 s, f) 0.001185 s, g) 0.0016 s, h) 0.00168 s, i) 0.001745 s. (contact area is represented with a stripe)

difficulties that would need to be overcome using appropriate methods (e.g. apriori mesh refinement in contact area [6]).

Bibliography

1. Atkinson K. E. Theoretical Numerical Analysis: A Functional Analysis Framework [3rd ed. ed.] / K. E. Atkinson, W. Han.– Springer, 2009. – P. 336-338.
2. Bergheau J.-M. Finite Element Simulation of Heat Transfer / J.-M. Bergheau, R. Fortunier. – Wiley-ISTE, 2008. – 302 p.
3. Chyr I. Computer simulation of friction hardering of superficial layers of machine details / I. Chyr, M. Jachymek, I. Hurey, V. Gurey, H. Shynkarenko // Manufacturing Processes. Some Problems.– Vol. 1. Basic science applications: M. Gajek, O. Hachkewych, A. Stanik-Besler eds.– Opole: Politechnika Opolska, 2012. – P. 49-62.
4. Hetch F. FreeFEM++ / F. Hetch.– // Electronic resource.– 2013. – [Cited 2013, 9 January].– Available from: http://www.freefem.org/ff++/ftp/freefem++doc.pdf.
5. Hurey I. V. Technological assurance of quality and exploitation properties details with parameters of impulse frictional processing: avtoref. dys. na zdobuttya nauk. stupenya d-ra tekhn. nauk: spets. 05.02.08 "Tekhnolohiya mashynobuduvannya" / I. V. Hurey.– Odesa, 2002. – 36 p. (in Ukrainian).
6. Kim C.-K. Adaptive finite element solution for the heat conduction with a moving heat source / C.-K. Kim // Journal of Mechanical Science and Technology. Springer.– 2012.– Vol. 26, № 3.– P. 967-972.
7. Malkin S. Thermal analysis of grinding / S. Malkin, C. Guo // CIRP Annals.– Manufacturing Technology.– Elsevier.– 2007.– Vol. 56, № 2.– P. 760-782.
8. Markopoulos A. P. Finite Element Method in Machining Processes / A. P. Markopoulos // SpringerBriefs in applied sciences and technology: Manufacturing and surface engineering.– Springer, 2013. – 92 p.
9. Mykhlyn S. H. Problema mynymuma kvadratychnoho funktsyonala / S. H. Mykhlyn.– Moscow: Hostekhyzdat, 1952. – 254 p. (in Russian).
10. Necas J. Mathematical theory of elastic and elasto-plastic bodies: an introduction / J. Necas, I. Hlavacek // Studies in Applied Mechanics.– Amsterdam:Elsevier Scientific Publishing Co., 1981. – Vol. 3.– 342 p.
11. Reznykov A. N. Teplofyzyka protsessov mekhanycheskoy obrabotky materyalov / A. N. Ryeznykov.– Moscow: Mashynostroenye, 1981. – 281 p. (in Russian).
12. Shynkarenko H. A. Proektsiyno-sitkovi skhemy rozvyazuvannya pochatkovo-krayovykh zadach / H. A. Shynkarenko.– Kyyiv: NMKVO, 1991. – 88 p. (in Ukrainian).
13. Vovk O. Projection grid scheme of carbon monoxide oxidation evolution models solutions on platinum surface / O. Vovk, N. Pavlenko, H. Shynkarenko, V. Vovk // Visnyk of Lviv University. Appl. Math. Comput. Science Series.– 2012.– Vol. 18.– P. 54-69 (in Ukrainian).

Ivan Chyr, Heorgiy Shynkarenko,
Ivan Franko National University of Lviv,
1, Universytets'ka Str., Lviv, 79000, Ukraine
Heorgiy Shynkarenko,
Opole University of Technology,
76, Proszkowska Str., Opole, 45-758, Poland

Received 4.11.2013